ELSEVIER

Journal of Photochemistry and Photobiology A: Chemistry 150 (2002) 177–185

Journal of Photochemistry and Photobiology A:Chemistry

www.elsevier.com/locate/jphotochem

A photochromic acceptor as a reversible light-driven switch in fluorescence resonance energy transfer (FRET)

L. Song [a,1], E.A. Jares-Erijman [a,b], T.M. Jovin [a,*]

[a] *Department of Molecular Biology, Max Planck Institute for Biophysical Chemistry, Am Fassberg 11, D-37077 Göttingen, Germany*
[b] *Departmento de Química Orgánica, Facultad de Ciencias Exactas y Naturales, Universidad de Buenos Aires, Ciudad Universitaria-Pabellón II, 1428 Buenos Aires, Argentina*

Received 8 October 2001; received in revised form 30 January 2002; accepted 25 February 2002

Abstract

A method has been developed for the quantitative determination of fluorescence resonance energy transfer (FRET) based on the modulation of donor fluorescence upon the reversible photoconversion of a photochromic acceptor. A model system was devised, consisting of Lucifer Yellow cadaverine (LYC, donor) conjugated to the photochromic molecule, 6-nitroBIPS (1′,3′-dihydro-1′-(2-carboxyethyl)-3′,3′-dimethyl-6-nitrospiro[2H-1-benzopyran-2,2′-(2H)-indoline]). Near-ultraviolet irradiation catalyzes the conversion of the colorless spiropyran (SP) to the colored merocyanine (MC) form of 6-nitroBIPS. Only the MC form absorbs at the emission wavelengths of the donor, thereby potentiating FRET, as demonstrated by quenching of the donor. Subsequent irradiation in the visible MC absorption band reverts 6-nitroBIPS to the SP form and FRET is inactivated. The acceptor exhibited high photostability under repeated cycles of alternating UV–Vis irradiation. In this model system, the intramolecular FRET efficiency was close to 100%. The observed maximal donor quenching of 34 ± 3% was indicative of an equilibrium determined by the high quantum efficiency of forward conversion (SP → MC) induced by near-UV irradiation and a low but finite quantum efficiency of the back reaction resulting from excitation of the MC form directly as well as indirectly (by FRET via the donor). A quantitative formalism for the photokinetic scheme was developed. Photochromic FRET (pcFRET) permits repeated, quantitative, and non-destructive FRET determinations for arbitrary relative concentrations of donor and acceptor and thus offers great potential for monitoring dynamic molecular interactions in living cells over extended observation times by fluorescence microscopy.

Keywords: Photochromism; Spiropyran; Merocyanine; Fluorescence microscopy; pcFRET

1. Introduction

In fluorescence resonance energy transfer (FRET), energy is transferred non-radiatively from an excited molecular fluorophore (donor) to another chromophore (acceptor) via intermolecular long-range dipole–dipole coupling [1]; for reviews see [2,3]. FRET occurs over a distance of 1–10 nm and its efficiency varies with the 6th power of the donor–acceptor separation. FRET microscopy [4–9] of biological structures offers three unique features: (a) one can resolve donor–acceptor distances with a resolution far exceeding the diffraction limit of optical microscopy; (b) the photophysical behavior of specific biomolecules labeled with the donor and acceptor reflects the static and dynamic properties of both intra- and inter-molecular interactions, including molecular proximity, complex formation, structural features, and microenvironment of the two molecular entities; (c) one can target specific intracellular components by co-expression as fusion proteins with green fluorescent protein (GFP) serving as indicators of concentration, interaction or localization [4–6,10–16].

The strategies for microscope measurements of FRET efficiency have been based on two different phenomena. (i) Sensitization of a fluorescent acceptor—manifested as an increase in its fluorescence upon excitation of the donor. In well-defined (usually intramolecular) single-donor single-acceptor systems, fluorescence ratio measurements involving different spectral components can be calibrated

Abbreviations: 6-NitroBIPS, 1′,3′-dihydro-1′-(2-carboxyethyl)-3′,3′-dimethyl-6-nitrospiro[2H-1-benzopyran-2,2′-(2H)-indoline]; LYC, Lucifer Yellow cadaverine, *N*-(5-aminopentyl)-4-amino-3,6-disulfo-1,8-naphthalimide; UV, ultraviolet light; Vis, light in the visible spectrum; FRET, fluorescence resonance energy transfer; pbFRET, photobleaching FRET; pcFRET, photochromic FRET; ^{1}H-NMR, proton nuclear magnetic resonance

* Corresponding author. Fax: +49-551-201-1467.
E-mail addresses: ls99@cornell.edu (L. Song), tjovin@gwdg.de (T.M. Jovin).
[1] Present address: School of Applied and Engineering Physics, Cornell University, 212 Clark Hall, Ithaca, NY 14852, USA.

1010-6030/02/$ – see front matter
PII: S1010-6030(02)00129-6

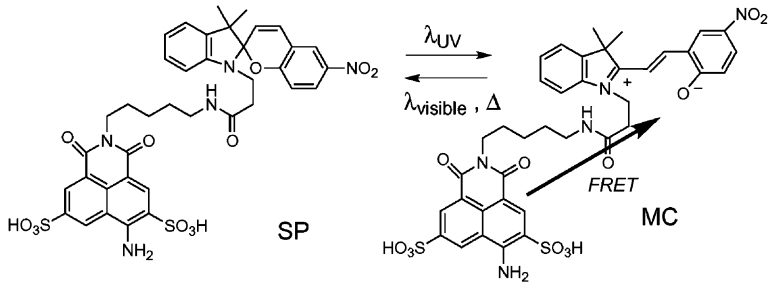

Fig. 1. Chemical structures of LYC–BIPS. The donor, LYC, is covalently linked to the photochromic molecule, 6-nitroBIPS. The most stable form of 6-nitroBIPS is the SP (left). Near-UV irradiation converts 6-nitroBIPS to the MC form (right), which acts as an energy acceptor for LYC. The MC form reverts to the SP form through the action of visible irradiation and in a spontaneous thermal reaction.

in terms of the FRET efficiency [9,17–22]. However, these techniques are difficult to implement in general because they require the acquisition and registration of three or more images. In addition, the acceptor must be fluorescent. (ii) Reduction of the donor fluorescence quantum yield (Q)—measurable through any of the four relationships given within the square brackets of the following equation:

$$\frac{Q^{DA}}{Q^{D}} \equiv (1-E) = \left[\frac{F^{DA}}{F^{D}} = \frac{\tau^{DA}_{decay}}{\tau^{D}_{decay}} = \frac{\tau^{D}_{bl}}{\tau^{DA}_{bl}} = \frac{F^{DA}(t=0)/\int_0^\infty F^{DA}(t)}{F^{D}(t=0)/\int_0^\infty F^{D}(t)} \right] \quad (1)$$

where E is FRET efficiency and the superscripts D and DA represent measurements of donor (D) characteristics in the absence and presence of acceptor (A), respectively. The first identity of Eq. (1) constitutes the master relationship for the FRET efficiency. A decrease of the steady-state emission intensity (F) and a reduction in the excited state lifetime (τ_{decay}) are the two classical measures of FRET. FRET can also be deduced from a decrease in the rate of photobleaching (τ_{bl}^{-1}) or in the initial intensity normalized by the time-integrated emission during photobleaching. The last two relationships in Eq. (1) were derived from analysis of the photobleaching properties of the donor and formed the basis of the pbFRET method introduced in 1989 [20,21].

The determination of E requires a reference state in which the acceptor is absent but the donor is otherwise in the same environment. The reference states (donor alone) are established either from a separate sample (experiment), or after selective photodestruction of the acceptor in situ or in another region of the same sample [4,7,23–27]. For static systems under cellular fixation, the pbFRET techniques are simple and useful [28–31]. However, photobleaching rates are linear or more complex [21] functions of irradiance and dependent on environmental parameters such as the local redox state [32,33]. In addition the photodestruction of donor or acceptor precludes the possibility of multiple FRET measurements at a given spatial location.

Our aim was to design a method that offers an intrinsic internal reference and the possibility for continued and repeated determinations of the FRET process. Photochromic compounds can be exploited to achieve this goal. Photochromism is the light-induced transformation of a single chemical species between two isomeric structures with distinct absorption spectra [34–37]. Near-ultraviolet irradiation induces reversible changes in the structure and absorption properties of a photochromic molecule from an initial colorless to a colored form. Only the latter has an absorption band overlapping the emission band of a selected donor and is thereby able to potentiate energy transfer. Subsequent irradiation in the visible absorption band of the colored form reverts it to the initial colorless form and disables the FRET process, thus supplying the required internal reference state. The FRET efficiency can be derived simply from the fractional change in donor fluorescence or donor lifetime for each pixel position. In this study, we chose 6-nitroBIPS from the relatively well-characterized spiropyran (SP) family [38] as the photochromic acceptor in a model molecular system designed to demonstrate the principle of pcFRET. A fluorescent donor, Lucifer Yellow cadaverine (LYC), was conjugated to 6-nitroBIPS (Fig. 1). We demonstrated through theoretical formalism and steady-state, kinetic, and time-resolved donor lifetime studies that switching the energy transfer process on and off can be achieved with this system, substantiating and extending preliminary observations [39]. The reversibility of pcFRET was evidenced by cyclical donor quenching/dequenching during alternations of UV–Vis irradiation.

We employ the terms Spiropyran (SP) and merocyanine (MC) when referring to the two isomeric forms of 6-nitroBIPS. Only the latter qualifies as the “acceptor.” The photoconversion from the SP to the MC form is referred to as forward photoconversion, and the light-induced reverse reaction as backward photoconversion. There is also a slow, spontaneous thermal reverse reaction in this system.

2. Experimental

2.1. Reagents, synthesis and analysis

1′,3′-Dihydro-1′-(2-carboxyethyl)-3′,3′-dimethyl-6-nitrospiro[2H-1-benzopyran-2,2′-(2H)-indoline] was obtained

from Chroma (McHenry, IL). We refer to this derivative of 6-nitroBIPS as 6-nitroBIPS throughout the paper. *N*-(5-aminopentyl)-4-amino-3,6-disulfo-1,8-naphthalimide (LYC) was from Molecular Probes (Eugene, OR). *N*,*N*′-dicyclohexyl-carbodiimide (DCC) and *N*-hydroxysuccinimide were purchased from Fluka (Fluka Chemie AG, Buchs, Switzerland). 6-Nitro-1′-(2-carboxyethyl) BIPS succinimidyl ester: 107 mg (0.2 mmol) of BIPS reacted with 120.3 mg (0.6 mmol) DCC and 74 mg (0.6 mmol) hydroxysuccinimide in 5 ml of dry acetonitrile at room temperature for 12 h. The precipitated dicyclohexylurea was filtered out and the BIPS succinimidyl ester dried in vacuo. LYC-6-nitroBIPS (LYC–BIPS): 2 mg (4 μmol) LYC was dissolved in a solvent mixture consisting of 280 μl DMF, 280 μl acetonitrile, and 160 μl 0.5 M Na-borate buffer (pH 9.2). Eight micromoles of the BIPS succinimidyl ester dissolved in dry acetonitrile, (excess) was reacted with 4 μmol LYC. The reaction was halted after 2 h by addition of 30 μl (excess) 1 M Tris–HCl buffer (pH 7.4). LYC–BIPS was isolated by HPLC using an RP-C18 column with an elution solvent mixture of acetonitrile and triethylammonium acetate buffer (1 M, pH 7.0) at a ratio of 35:65 (v/v), in an isocratic mode. The conjugation and identity of LYC–BIPS were confirmed by ^{1}H-NMR and electrospray mass spectroscopy.

^{1}H-NMR (300 MHz, CD_3OD) δ: 9.05 (1H, d, 1.5 Hz, H-7 LYC); 8.90 (1H, d, 1.5 Hz, H-5 LYC); 8.88 (1H, s, H-2); 8.10 (1H, d, 3 Hz, H-5 BIPS); 8.00 (1H, dd, 8.5 and 3 Hz, H-7 BIPS); 7.10 (1H, dt, 3 and 8.7 Hz, H-12 BIPS); 7.06 (1H, d, 10.5 Hz, H-4 BIPS); 7.02 (1H, d, 8.7 Hz, H-14 BIPS); 6.75 (1H, d, 8.5 Hz, H-8 BIPS); 6.77 (1H, t, 8.7 Hz, H-13 BIPS); 6.65 (1H, d, 8.7 Hz, H-11 BIPS); 5.96 (1H, d, 10.5 Hz, H-3 BIPS); 4.6 (1H, broad s, N*H*); 4.05 (2H, m, NCH_2CCCCNHCO); 3.75 (2H, m, NCCCCCH_2NHCO); 2.54, 2.52 (2H, m, COCH_2CN); 1.22 (3H, s, CH_3 BIPS); 1.15 (3H, s, CH_3 BIPS). The ^{1}H-NMR signals at 9.05, 8.90, and 8.88 ppm (LYC H-7, H-5 and H-2) and at 8.10 and 8.00 ppm (H-5 and H-7 BIPS) integrated with a ratio of 1:1:1:1:1. A triplet at 3.75 ppm was assigned to CH_2NHCO. The signal at 2.80 ppm characteristic for CH_2NH$_2$ in free LYC was absent.

2.2. Photoconversion

The light source for photochromic conversion was a 200 W DC super-pressure short arc mercury lamp coupled to a liquid lightguide with high UV transmission (Lumatec GmbH, Munich, Germany). A near-UV bandpass filter (320–380 nm) was used for forward photoconversion, and a green filter (520–580 nm) for backward photoconversion. The maximum irradiance was 1.8 W cm^{-2} at 365 nm and 1.1 W cm^{-2} at 547 nm (estimated for the spectral band about the central wavelength). Unless otherwise indicated, all forward photoconversions were accomplished with the 320–380 nm band, and the backward photoconversion using the 520–580 nm band at the maximum irradiance.

2.3. Steady-state spectroscopy

Steady-state absorption spectra of LYC–BIPS were acquired at 22 °C and with 1 nm resolution in a Uvikon spectrophotometer (Model 943, Kontron Instruments, Milan, Italy). Steady-state fluorescence measurements were performed at 22 °C with 1 nm resolution in a Model 8000S spectrofluorimeter (SLM Instruments, Urbana-Champaign, IL). The emission spectra were corrected for instrument response, lamp fluctuations and solvent background contributions. Polarization effects were suppressed by use of "magic angle" conditions. Emission spectra were collected in the 470–700 nm range with excitation at 430 nm (donor), using constant slit apertures and gain settings. Unless otherwise indicated, measurements were in sealed quartz cuvettes with an optical pathlength of 5 mm. The steady-state spectra were used to estimate the probability of energy transfer. The Förster distance, R_0, at which the energy transfer rate is equal to the intrinsic donor decay rate, is given by $R_0^6 = 8.8 \times 10^{-5}\kappa^2\Phi_D J n^{-4}$ (units, Å^6), where Φ_D is the quantum yield of the donor in the absence of acceptor, n is the refractive index of the medium, κ^2 is the orientation factor between donor and acceptor transition moments (assumed to be $\frac{2}{3}$, valid for rapidly reorienting donor and acceptor), and J is the integral expressing the overlap between the donor emission and acceptor absorption; $J = \int F_\lambda^D \varepsilon_\lambda^A \lambda^4 \, d\lambda$, where F_λ^D is the normalized donor fluorescence spectrum and ε_λ^A is the molar absorption coefficient (M^{-1} cm^{-1}) of the acceptor at wavelength λ (nm).

2.4. Kinetic spectroscopy

Absorption and fluorescence kinetic measurements were performed with a stopped-flow system (Model SX.18MV, Applied Photophysics, Leatherhead, UK). The 2 × 1 × 10 mm flow cell was adapted for dual light sources, with the photoconversion light path perpendicular to the detection path (10 and 1 mm for absorption and fluorescence, respectively). Absorption and fluorescence (MC form) were measured at 535 and 530 ± 3 nm, respectively; excitation of fluorescence was by the combination of the near-UV irradiation and a 430 ± 6 nm source. The forward and backward conversions were initiated by 320–380 and 520–580 nm irradiation, respectively.

2.5. Fluorescence lifetime

Donor fluorescence lifetimes were determined with a frequency-domain lifetime system [40]. A deuterium light source (Cathodeon, Cambridge, UK) was modulated at 10–110 MHz [41]. The reference was 10 μM fluorescein in 95% EtOH, 5% 1 mM NaOH; $\tau_f = 4.13$ ns [42]. The excitation band was selected with a 310 nm or a 450 nm bandpass filter and the emission collected at >520 nm. Both phase shift and modulation depth were recorded and analyzed with the program Globals Unlimited (University of

Illinois at Urbana-Champaign, IL). A single discrete lifetime model sufficed for fitting the decay curves of both LYC–BIPS and LYC–MC samples.

3. Results and discussion

3.1. LYC–BIPS, a model system for pcFRET

LYC was selected as the donor for the photochromic acceptor for two reasons: (i) at its absorption maximum, the absorbances of the SP and MC forms of 6-nitroBIPS are minimal; (ii) the LYC emission spectrum coincides with the absorption peak of the MC form (Fig. 2).

For the donor–acceptor pair LYC and MC, the Förster transfer distance R_0 was calculated as 30–40 Å. The distance, r, between the central carbon atoms of the donor and the MC acceptor of the energy minimized structure was ~13 Å. The FRET efficiency, based on these values in the relationship $E = [1+(r/R_0)^6]^{-1}$ is >0.99, and would increase further if intramolecular diffusional donor–acceptor reorientation occurs during the excited state lifetime.

3.2. Photokinetic modeling

The photochromic FRET (pcFRET) system is photophysically bistable. When the SP form is photoconverted to the MC form, the change in the absorption spectrum and consequent increase in the overlap integral J (and thus in R_0) potentiates the FRET process (the ON state). Reversion of the MC form to the SP form upon light exposure or by spontaneous (thermal) reaction turns FRET OFF. The

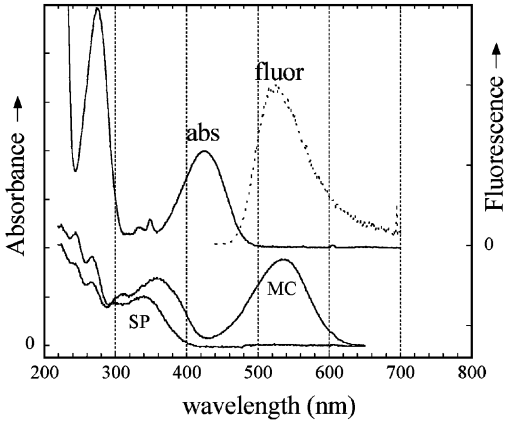

Fig. 2. Absorption and emission spectra of the donor LYC and photochromic acceptor in its ON and OFF states. Left axis: absorbances of the donor (displaced upward), and of the SP and MC forms of 6-nitroBIPS. Right axis: fluorescence spectrum of the donor excited at 430 nm. Note that there is no overlap between the donor fluorescence emission spectrum and the absorption spectrum of the SP form (OFF state). After near-UV irradiation, the overlap between the donor emission and the absorption spectrum of the MC form enables the FRET process (ON state). Irradiation at the absorption maximum of the MC form reverts 6-nitroBIPS to the initial SP form.

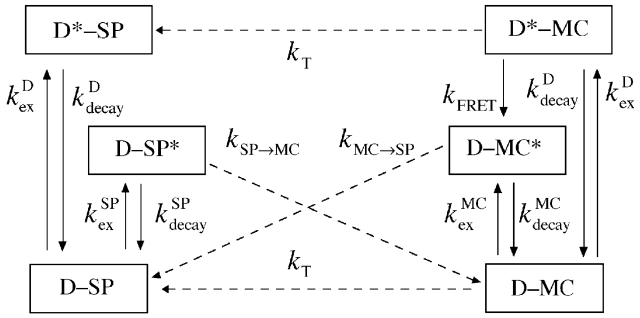

Fig. 3. Photokinetic model for pcFRET. Each rectangular box denotes a given molecular species in which a donor is covalently linked to the photochromic acceptor. The abbreviations D, SP and MC refer to donor, SP and MC moieties, respectively. The ground-state species are D-SP and D-MC, and their respective excited-state species D*-SP, D-SP*, D*-MC and D-MC*. The asterisk (*) denotes the singlet excited state. The rate constants are defined by a superscript and subscript denoting a given molecular moiety and the associated photophysical process, respectively. Dashed arrows indicate that a process is not necessary a single elementary step and may involve transient intermediates. $k_{SP\to MC} = 1\times10^{11}\,s^{-1}$ [46,47]; $k_{MC\to SP} = 80k_{decay}^{MC}$, derived from the fluorescence quantum yield for MC* in ethanol 0.012 [43]; $k_{decay}^{MC} = 2.5\times10^{9}\,s^{-1}$ [43,47,48]; $k_{decay}^{SP} = 5\times10^{11}\,s^{-1}$, based on the quantum yield of photocoloration, albeit of a benzothiazolinic SP, $\Phi_{SP} = 0.15\pm0.03$ [49]; $k_T = 6.5\times10^{-4}\,s^{-1}$ and $\tau^D = 4.0\times10^{-9}$ s were measured in this study; $k_{FRET} = k_{decay}^{D}(R_0/r)^6$, where $R_0 = 30$ Å, $r = 13$ Å (see text). The only input variables in the simulation are k_{ex}^{D}, k_{ex}^{SP}, and k_{ex}^{MC}, the rate constants for absorption (excitation), proportional to the product of the molar extinction coefficient ($M^{-1}\,cm^{-1}$) and the irradiance I ($W\,cm^{-2}$) at a given wavelength λ (nm); $k_{ex} = 7.6\times10^{-6}\varepsilon_i\lambda I$. The extinction coefficients are: $\varepsilon_{426\,nm}^{D} = 11{,}000\,M^{-1}\,cm^{-1}$ [50], $\hat{\varepsilon}_{320-380\,nm}^{D} \approx 4000\,M^{-1}\,cm^{-1}$, derived from spectral data, $\varepsilon_{300\,nm}^{SP} = 17{,}000\,M^{-1}\,cm^{-1}$ and $\varepsilon_{530\,nm}^{MC} = 28{,}000\,M^{-1}\,cm^{-1}$ [44,51]. For completeness and symmetry, a FRET D* → SP* transition could be included although such a step was not operative in the system under study.

factors determining the equilibrium are the wavelength and irradiance of the photoconversion light that is absorbed by the photochromic moiety and to some extent by the donor. The kinetic formulation presented below was designed to explore the conditions that determine the equilibrium photostationary state and to optimize experimental design.

The generalized photokinetic scheme (Fig. 3) takes into account the main reaction steps but omits photodegradation processes or the intervention of doubly excited species. Key parameters were deduced in part from the known properties of a closely related 6-nitroBIPS analog (1′,3′-dihydro-1′,3′,3′-trimethyl-6-nitro-Spiro[2H-1-benzopyran-2,2′-[2H]indole], CAS Registry No. 1498-88-0). The resulting system of differential equations corresponding to the photokinetic scheme was first solved by numerical integration. The results indicated that intermediates occur at very low fractional concentration and all excited-state species are rapidly depopulated. Thus, analytical solutions were derived based on the assumption of steady-state equilibria, indicating that the system of Fig. 3 reduces to an exchange reaction between the two ground-state species D–SP and D–MC. Symbolic and numerical manipulations

of the equations using *Mathematica* (Wolfram Research) yielded the following wavelength-dependent relationships.

$$\text{D–SP} \underset{k_{OFF}}{\overset{k_{ON}}{\rightleftharpoons}} \text{D–MC} \tag{2}$$

$$k_{ON} = k_{ex}^{SP} Q_{SP\rightarrow MC},$$
$$k_{OFF} = (k_{ex}^{MC} + k_{ex}^{D} E_{FRET}) Q_{MC\rightarrow SP} + k_T(1 + \gamma^{MC}) \tag{3}$$

$$Q_{SP\rightarrow MC} = \frac{k_{SP\rightarrow MC}}{k_{SP\rightarrow MC} + k_{decay}^{SP}},$$
$$Q_{MC\rightarrow SP} = \frac{k_{MC\rightarrow SP}}{k_{MC\rightarrow SP} + k_{decay}^{MC}} \tag{4}$$

$$E_{FRET} = \frac{k_{FRET}}{k_T + k_{decay}^{D} + k_{FRET}} \approx \frac{k_{FRET}}{k_{decay}^{D} + k_{FRET}},$$
$$\gamma^{MC} = \frac{[\text{D}^*\text{–MC}]}{[\text{D–MC}]} \approx \frac{k_{ex}^{D}}{k_{decay}^{D} + k_{FRET}} \tag{5}$$

The overall rate constants are designated as k_{ON} and k_{OFF} to emphasize the reaction pathways turning the FRET process ON and OFF, respectively. The various quantum yields (Q_i and E_{FRET}) and the donor excited-state/ground-state equilibrium (γ^{MC}, most generally of negligible magnitude for operation far from saturation) in Eqs. (3)–(5) reflect the distribution between branches in the reaction pathway. The only rate constants defining the kinetics of the system are those for excitation and the thermal return from the MC to the SP form.

The dependence of the equilibrium state on the excitation level of SP and MC is shown in Fig. 4A and B. The population of the MC species increases monotonically with k_{ex}^{SP} and decreases with k_{ex}^{MC}. For a FRET efficiency close to unity (our model system), both k_{ex}^{MC} and k_{ex}^{D} contribute equally to the overall rate of backward photoconversion (Fig. 3 and the first term of Eq. (5)), corresponding to the two parallel pathways, (D–MC → D–MC* → D–SP) and (D–MC → D*–MC → D–MC* → D–SP), respectively. The rate of the spontaneous thermal backward reaction (k_T in Fig. 3) varies widely depending on the substituents and polarity of solvent, even within the SP family [43,44]. For 6-nitro BIPS under our experimental conditions, the reaction was slow ($k_T = 0.032\,\text{min}^{-1}$) and thus of significance only in the absence of light and as a determinant of long-term stability.

The kinetics of re-equilibration upon changing the excitation conditions (wavelength, irradiance) is monoexponential (rate constant = $k_{ON} + k_{OFF}$), as represented in the following expression for the fraction of the photochromic

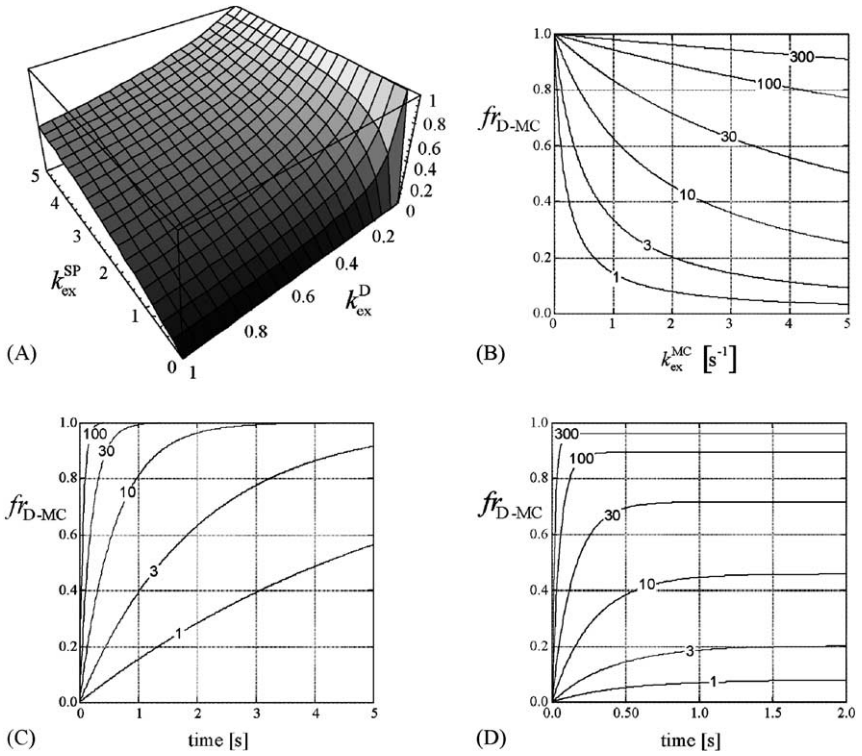

Fig. 4. Mathematical simulations of pcFRET. (A) Fraction of photochromic 6-nitroBIPS acceptor in the D-MC form at equilibrium ($fr_{D\text{-}MC}$) as a function of the excitation rates k_{ex}^{SP} and k_{ex}^{D} (s^{-1}); $k_{ex}^{D} = 0$. Other constants (s^{-1}): photodeactivation ($k_{decay}^{SP} = 5 \times 10^{11}$, $k_{decay}^{MC} = 2.5 \times 10^{9}$, k_{decay}^{D}=2.44×10^{8}); photochromism ($k_{SP\rightarrow MC} = 1 \times 10^{11}$, $k_{MC\rightarrow SP} = 80 k_{decay}^{MC}$, $k_T = 6.5 \times 10^{9}$); FRET ($k_{FRET} = [30/13]^6 k_{decay}^{D}$). (B) $fr_{D\text{-}MC}$ as a function of k_{ex}^{MC} and increasing values of k_{ex}^{SP} (1–300). (C) Time course of $fr_{D\text{-}MC}$ for different values of k_{ex}^{SP} (1–100); k_{ex}^{MC} and $k_{ex}^{D} = 0$. (D) Time course of $fr_{D\text{-}MC}$ for different values of k_{ex}^{SP} (1–300) and for $k_{ex}^{MC} = k_{ex}^{D} = 1$. See text for interpretations.

compound in the MC form (D–MC):

$$fr(t)_{\text{D–MC}} = \frac{k_{\text{ON}} + [k_{\text{OFF}}\alpha - k_{\text{ON}}(1-\alpha)]\,\mathrm{e}^{-(k_{\text{ON}}+k_{\text{OFF}})t}}{k_{\text{ON}} + k_{\text{OFF}}} \tag{6}$$

The initial state is given by $fr(0)_{\text{D–MC}} = \alpha$ and the final photostationary equilibrium state by

$$fr(\infty)_{\text{D–MC}} = \frac{k_{\text{ON}}}{k_{\text{ON}} + k_{\text{OFF}}} \tag{7}$$

These features are illustrated in Fig. 4C and D. Starting from a population entirely in the SP form (at thermal equilibrium and in the absence of irradiation, $\alpha = 0$ for the MC–SP system), excitation leads to conversion to the MC state with a rate (panel C) and to an extent (panel D) that increase with $k_{\text{ex}}^{\text{SP}}$ (for fixed values of $k_{\text{ex}}^{\text{MC}}$ and k_{ex}^{D}) in accordance with Eqs. (3), (6) and (7).

Excitation at a wavelength absorbed by all three species (D, SP, MC; panel D) initiates parallel reactions leading to an equilibrium state characterized by an incomplete conversion of SP to MC because $k_{\text{OFF}} \neq 0$ (Eqs. (3) and (6)). These different cases show that the dynamic range available for the pcFRET system is determined by the available irradiances and the degree of selectivity with which the two photochromic states can be activated by light. This property is easy to achieve in the visible region (for inducing backward photoconversion) but is more difficult in the near-UV (for forward photoconversion), where most organic compounds absorb. Nonetheless, for 6-nitroBIPS, the interconversion between SP and MC with near UV [45] strongly favors the MC form (see values of $Q_{\text{SP}\rightarrow\text{MC}}$ and $Q_{\text{MC}\rightarrow\text{SP}}$; Eq. (4), Fig. 4).

The excited-state species in Fig. 3 never achieved fractional concentrations higher than 10^{-8} in the simulations, although conceivably the relatively long-lived excited state of the donor could be saturated. However, in practice donor excitation is maintained at the lowest level compatible with a suitable (from a signal-to-noise standpoint) analytical determination of $fr_{\text{D-MC}}$ during a kinetic process or at equilibrium. The underlying assumption is that changes in the donor fluorescence quantum yield arise solely from the FRET process. Thus, the quenching of the donor can be expressed as a function of $fr_{\text{D-MC}}$ and the FRET efficiency:

$$\begin{aligned}\text{quenching}_{\text{D}} &= 1 - [(1 - fr_{\text{D–MC}}) + fr_{\text{D–MC}}(1 - E_{\text{FRET}})] \\ &= E_{\text{FRET}} fr_{\text{D-MC}}\end{aligned} \tag{8}$$

It follows that for $E_{\text{FRET}} \approx 1$, $\text{quenching}_{\text{D}} = fr_{\text{D–MC}}$.

3.3. Steady-state cyclical spectroscopy

The LYC–BIPS concentration was adjusted to maintain the absorbances at 0.02–0.07 (path length 0.5 cm) to avoid inner filter effects. Prior to near-UV irradiation, the photochromic moiety was in its initial, most stable SP form and

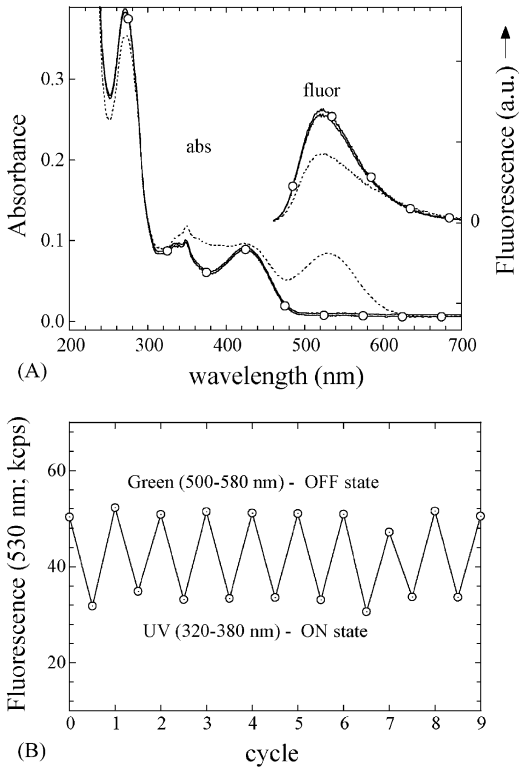

Fig. 5. Absorption and fluorescence spectra during cyclical SP-MC photochromic transitions of LYC–BIPS. (A) Absorption spectra and donor fluorescence spectra (excitation 430 nm) of LYC–BIPS in methanol before exposure to any irradiation (—), after UV (320–380 nm) irradiation at 1.8 W cm^{-2} for 7 s (···), and after visible (520–580 nm) irradiation at 1.1 W cm^{-2} for 15 s (—○—). First cycle data. (B) Ten continuous cycles monitored by fluorescence.

the donor fluorescence was at a maximum (Fig. 5A). After exposure to near-UV light, formation of the MC form and the simultaneous decrease of the SP form were reflected by the changes in absorbance at 500–600 nm (increase) and at 270 nm (decrease). Thus, the photochromic moiety was converted to a FRET acceptor (ON state). The donor fluorescence showed a concomitant decrease (Fig. 5A). Upon exposure to green light for 15 s, the absorption and fluorescence spectra returned to their initial values, indicating that the MC form had reverted to the SP form. That is, the photochromic moiety no longer acted as an energy acceptor (OFF state). Fig. 5 represents a typical experiment in which the UV–Vis cycle was repeated 10 times and monitored by fluorescence (Fig. 5B). In this particular data set, the forward photoconversion led to an increase in A_{530} (MC) of 0.065 ± 0.004, a decrease in A_{270} (SP) of 0.042 ± 0.002, and a decrease in the donor fluorescence intensity by 34% ($\pm$3%, $N = 10$).

The concomitant changes in the absorbance of the photochromic acceptor and in the fluorescence of the donor induced by the UV–Vis irradiation cycles constituted a direct demonstration of pcFRET. The decrease in the SP form monitored by A_{270} was paralleled by an increase in the MC form monitored at A_{530} and by changes in donor

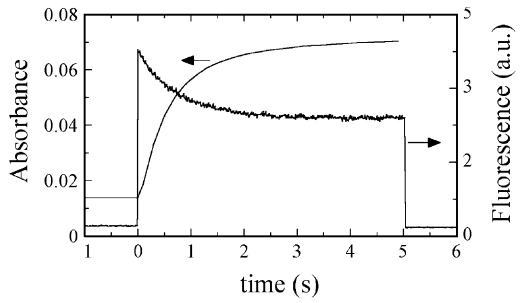

Fig. 6. Absorption and fluorescence kinetics during forward photoconversion from the SP to the MC form. Near-UV irradiation at 320–380 nm (0.6 W cm^{-2}). Absorption kinetics monitored at 535 nm. Donor fluorescence monitored at its maximum (530 nm) with excitation at 430 nm. In the fluorescence experiment, the near-UV photoconversion light source was turned on for 5 s.

fluorescence emission. The latter decreased by 34% upon near-UV irradiation but reverted to its original following photoreversion induced by visible (green) light. We excluded inner filter effects, trivial reabsorption, and photodegradation as processes accounting for the observations. For example, control samples (donor alone) treated under the same experimental conditions showed a constant emission. A ground-state donor–acceptor complex was not involved in the quenching in view of the invariant absorption (430 nm) and fluorescence (530 nm) peaks of LYC before and after conjugation to the photochromic moiety.

The absorption spectrum of D–SP species could be measured directly on a previously dark-stored sample, and scanned from long to short wavelengths. The absorption spectrum of the pure D–MC species was determined by taking advantage of its virtually 100% FRET efficiency, such that donor quenching is directly proportional to the fractional molecular population of the D–MC form. The D–MC absorption spectrum has absorption maxima at 270 and 370 in addition to 530 nm. The finite absorption of both MC and the donor in the near-UV implies that the back reaction is also photoinduced to a certain degree (Eq. (5)). In fact, this circumstance defines the photostationary equilibrium state achieved under any specific condition. It follows that the donor–acceptor conjugate photoconverts to slightly lesser degree (upon near-UV irradiation) than SP-6-nitroBIPS alone.

3.4. Kinetic spectroscopy

The formation of the MC form was studied by absorption kinetics (at 530 nm, Fig. 6) as a function of the near-UV irradiance to determine the relevant rate constants and the conditions maximizing the dynamic range (degree of conversion). The absorbance increased as the MC form was generated under constant illumination. Analysis of the absorbance traces yielded results similar to those of fluorescence (see below), but there were slight deviations from strictly mono-exponential behavior attributable to a non-optimal geometry (the photolyzed volume was smaller than the measured volume) and a possible stray light signal originating from the donor fluorescence. The equilibration rate constant was linearly dependent on the irradiance over a 25-fold range, but the degree of conversion (to the final photostationary state) achieved a maximal value (34–36%), in accordance with Eqs. (3) and (7).

The donor fluorescence kinetics was monitored under the same conditions (Fig. 6). At the instant of turning on the near-UV source, the signal at 530 nm was at a maximum, then decreased exponentially to a constant level as the system attained equilibrium. The rate constant was $1.4 \pm 0.1\ s^{-1}$ and the relative amplitude (fractional decrease) $36 \pm 2\%$ (means and S.D. from three experiments), in good agreement with the value from the steady-state measurement (34%). Various control measurements (solvent, BIPS and LYC alone) confirmed that the near-UV exposure to each individual chemical component did not lead to either photobleaching of the donor, a new fluorescent species, or a perceptible fluorescence kinetic process.

The kinetics of the backward reaction induced by green light were also studied (data not shown). In the absence of light and at room temperature, the MC form reverted spontaneously to the SP form in a slow, first-order process [38] with a rate constant (k_T) of 0.032 min^{-1}.

3.5. Donor fluorescence lifetimes

The donor fluorescence lifetimes of LYC–SP and LYC–MC were determined by the frequency-domain method. The observed lifetimes of both molecular forms measured at the donor emission wavelength were the same: 4.04 ± 0.05 ns. Based on the fundamental relationships in Eq. (1), the relative change in donor lifetime should be equal to fractional quenching of the donor. The molecular model system in this study presented a special case in as much as the intra-molecular FRET process was calculated to have a transfer efficiency close to 100%. Thus, the donor fluorescence from the fractional population undergoing FRET would be quenched completely, such that the observed donor fluorescence lifetime would correspond exclusively to the fractional population D–SP, i.e. the molecules not undergoing FRET. At the same time, the degree of donor quenching would reflect the fractional population of D-MC. In the general case, where donor and acceptor are not directly coupled to each other (via a spacer), but to biomolecule(s) of interest, the donor fluorescence will not be completely quenched (Eq. (1)) and a second component with a distinct lifetime should be discernible.

4. Conclusions and perspectives

The process of energy transfer from a fluorescent donor to a photochromic acceptor, as evidenced through donor fluorescence quenching, can be switched on and off by

photo-induced conversion between the colorless and colored forms of the photochromic molecule. The current model system, in which a donor and an acceptor molecule were covalently linked, yielded an energy transfer efficiency close to 100%. The donor fluorescence quenching and related theoretical analysis demonstrate that the equilibrium between the forward photochromic conversion and the reverse reaction is dictated by: (i) the relative absorption spectra of the two forms of the photochromic moiety; (ii) the extent to which donor-mediated energy transfer contributes to photoreversion, and (iii) the respective quantum yields for the two opposing reactions. The extremes of the fractional population of D–SP and D–MC define the dynamic range of the observed fluorescence. To achieve a complete conversion of the colorless to the colored form, the wavelength for photochromic conversion should be in the spectral region in which the donor and the colored form do not absorb, a requirement that is difficult to fulfill in practice. The present study of pcFRET involved the spectroscopy of solutions, but the most important anticipated applications will be in microscopy. Conjugation of photochromic moieties to biomolecules and donor fluorescence modulation through interconversion of the photochromic isomers has been achieved and will be reported elsewhere. In addition, photochromic diarylethenes that do not exhibit thermal reversion have been investigated for suitability in pcFRET (L. Giordano, M. Irie, T.M. Jovin, and E. A. Jares-Erijman, unpublished data).

The photoreversibility of the photochromic acceptor offers a unique opportunity for performing repeated quantitative FRET observations under the unknown stoichiometry of the donor–acceptor relationships prevailing in microscopy experiments. A photochromic acceptor offers the critical internal control (acceptor-free donor) within the same sample preparation and at every spatial location and chemical environment. In studies of living cells, it may be possible to circumvent the need for exposure to potentially phototoxic near-UV irradiation by application of multiphoton excitation. The pcFRET strategy can be extended to nucleic acid or intramolecular protein-based FRET probes, analogous to the visible fluorescent proteins such as GFP, which are capable of adopting distinct molecular conformations and in studies of dynamic processes requiring triggering by light.

Acknowledgements

L. Song thanks T. Visser, A. van Hoek, N. Visser, K. Zachariasse and S. Druzhinin for helpful discussions and preliminary time-domain lifetime experiments; R. Clegg and G. Striker for helpful discussions; Q. Hanley and R. van Gorsel for critical reading of the manuscript. The authors also thank G. Heim for laboratory assistance. L. Song was a recipient of a Marie Curie post-doctoral fellowship of the European Commission TMR Program. This work was supported by the Max Planck Society, and in part by grant I/77897 from the Volkswagen Foundation to E.A. Jares-Erijman and T.M. Jovin.

References

[1] T. Förster, Discuss. Faraday Soc. 27 (1959) 7.
[2] R.M. Clegg, in: X.F. Wang, B. Herman (Eds.), Chemical Analysis Series, Vol. 137, Wiley, New York, 1996.
[3] P.R. Selvin, Method. Enzymol. 246 (1995) 300.
[4] J. Lippincott-Schwartz, E. Snapp, A. Kenworthy, Nat. Rev. Mol. Cell Biol. 2 (2001) 444.
[5] J. Goedhart, T.W.J. Gadella, in: R.W. Ridge, A.M.C. Emons (Eds.), Root Hairs: Cell and Molecular Biology, Springer, Tokyo, 2000.
[6] P.R. Selvin, Nat. Struct. Biol. 7 (2000) 730.
[7] A.K. Kenworthy, M. Edidin, Method. Mol. Biol. 116 (1999) 37.
[8] P.I.H. Bastiaens, T.M. Jovin, in: J.E. Celis (Ed.), Cell Biology: A Laboratory Handbook, Vol. 3, 2nd Edition, Academic Press, New York, 1998.
[9] G.W. Gordon, G. Berry, X.H. Liang, B. Levine, B. Herman, Biophys. J. 74 (1998) 2702.
[10] M.R. Hanson, R.H. Kohler, J. Exp. Bot. 52 (2001) 529.
[11] A.G. Harpur, F.S. Wouters, P.I. Bastiaens, Nat. Biotechnol. 19 (2001) 167.
[12] C. Chamberlain, K.M. Hahn, Traffic 1 (2000) 755.
[13] A. Miyawaki, R.Y. Tsien, Method. Enzymol. 327 (2000) 472.
[14] T.W.J. Gadella, G.N.M. van der Krogt, T. Bisseling, Trends Plant Sci. 4 (1999) 287.
[15] R. Heim, Method. Enzymol. 302 (1999) 408.
[16] B.A. Pollok, R. Heim, Trends Cell Biol. 9 (1999) 57.
[17] S.R. Adams, A.T. Harootunian, B. Ying Ji, S.S. Taylor, R.Y. Tsien, Nature 349 (1991) 694.
[18] R.M. Clegg, Method. Enzymol. 211 (1992) 353.
[19] E.A. Jares-Erijman, T.M. Jovin, J. Mol. Biol. 257 (1996) 597.
[20] T.M. Jovin, D.J. Arndt-Jovin, Annu. Rev. Biophys. Biophys. Chem. 18 (1989) 271.
[21] T.M. Jovin, D.J. Arndt-Jovin, in: E. Kohen, J.G. Hirschberg, J.S. Ploem (Eds.), Cell Structure and Function by Microspectrofluorometry, Academic Press, London, 1989.
[22] K. Luby-Phelps, F. Lanni, D.L. Taylor, Annu. Rev. Biophys. Biophys. Chem. 17 (1988) 369.
[23] P.I.H. Bastiaens, I.V. Majoul, P.J. Verveer, H.D. Söling, T.M. Jovin, EMBO J. 15 (1996) 4246.
[24] R. Varma, S. Mayor, Nature 394 (1998) 798.
[25] F.S. Wouters, P.I. Bastiaens, K.W. Wirtz, T.M. Jovin, EMBO J. 17 (1998) 7179.
[26] F.S. Wouters, P.I.H. Bastiaens, Curr. Biol. 9 (1999) 1127.
[27] A.K. Kenworthy, N. Petranova, M. Edidin, Mol. Biol. Cell 11 (2000) 1645.
[28] P.I.H. Bastiaens, T.M. Jovin, Proc. Natl. Acad. Sci. USA 93 (1996) 8407.
[29] G. Szabo Jr., J.L. Weaver, P.S. Pine, P.E. Rao, A. Aszalos, Biophys. J. 68 (1995) 1170.
[30] F.S. Wouters, P.I.H. Bastiaens, K.W.A. Wirtz, T.M. Jovin, EMBO J. 17 (1998) 7179.
[31] R.M. Young, J.K. Arnette, D.A. Roess, B.G. Barisas, Biophys. J. 67 (1994) 881.
[32] L. Song, E. Hennink, I.T. Young, H.J. Tanke, Biophys. J. 68 (1995) 2588.
[33] L. Song, C.A.G.O. Varma, J.W. Verhoeven, H.J. Tanke, Biophys. J. 70 (1996) 2959.
[34] J.C. Crano, R.J. Guglielmetti (Eds.), Organic Photochromic and Thermochromic Compounds, Vol. 1, Kluwer Academic Publishers/Plenum Press, New York, 1999.
[35] J.C. Crano, R.J. Guglielmetti (Eds.), Organic Photochromic and Thermochromic Compounds, Vol. 2, Kluwer Academic Publishers/Plenum Press, New York, 1999.

[36] H. Dürr, H. Bouas-Laurent (Eds.), Photochromism: Molecules and Systems, Elsevier, Amsterdam, 1990.
[37] M. Irie, Chem. Rev. 100 (2000) 1685.
[38] R. Guglielmetti, in: H. Dürr, H. Bouas-Laurent (Eds.), Photochromism: Molecules and Systems, Elsevier, Amsterdam, 1990.
[39] E. Jares-Erijman, L. Song, T.M. Jovin, Mol. Cryst. Liq. Cryst. 298 (1997) 151.
[40] T.W.J. Gadella Jr., T.M. Jovin, R.M. Clegg, Biophys. Chem. 48 (1993) 221.
[41] C.G. Morgan, Y. Hua, A.C. Mitchell, J.G. Murray, A.D. Boardman, Rev. Sci. Instrum. 67 (1996) 41.
[42] J. Baumann, G. Calzaferri, L. Forss, T. Hugentobler, J. Photochem. 28 (1985) 457.
[43] A.K. Chibisov, H. Görner, J. Photochem. Photobiol. A 105 (1997) 261.
[44] H. Görner, Chem. Phys. 222 (1997) 315.
[45] Y. Atassi, J.A. Delaire, K. Nakatani, J. Phys. Chem. 99 (1995) 16320.
[46] N.P. Ernsting, Chem. Phys. Lett. 159 (1989) 526.
[47] S.A. Krysanov, M.V. Alfimov, Chem. Phys. Lett. 91 (1982) 77.
[48] K. Horie, K. Hirao, I. Mita, Y. Takubo, T. Okamoto, M. Washio, S. Tagawa, Y. Tabata, Chem. Phys. Lett. 119 (1985) 499.
[49] A. Samat, J. Kister, F. Garnier, J. Metzger, R. Guglielmetti, Bull. Soc. Chim. Fr. (1975) 2627.
[50] R.P. Haugland, Handbook of Fluorescent Probes and Research Chemicals, 6th Edition, Molecular Probes Inc., Eugene, Oregon, 1998.
[51] V. Pimienta, D. Lavabre, G. Levy, A. Samat, R. Guglielmetti, J.C. Micheau, J. Phys. Chem. 100 (1996) 4485.